scientific reports

Check for updates

OPEN

Targeted co-delivery nanosystem based on methotrexate, curcumin, and PAMAM dendrimer for improvement of the therapeutic efficacy in cervical cancer

Ayuob Aghanejad[1,8], Shiva Kheiriabad[2,8], Maryam Ghaffari[3], Simin Namvar Aghdash[2], Neda Ghafouri[3], Jafar Ezzati Nazhad Dolatabadi[4]✉, Hashem Andishmand[5,6]✉ & Michael R. Hamblin[7]✉

The simultaneous administration of multiple drugs within identical nanocarriers to cancer cells or tissues can result in the effective action of drugs at reduced concentrations. In this investigation, PAMAM dendrimers (G4-PAMAM) were employed to link with methotrexate (MTX) using DCC/NHS chemistry and followed by the entrapment of curcumin (Cur) within it. The establishment of covalent bonds between MTX and the PAMAM dendrimer led to PAMAM-MTX interaction, verified and described through FT-IR. Various techniques were employed to evaluate the structural properties of the prepared Cur-PAMAM-MTX NC. The Cur-PAMAM-MTX NC, after preparation, exhibited a particle size of 249 nm, with an encapsulation efficiency (EE) of ~ 81% for Cur. The cumulative in vitro release of Cur-loaded NC indicated a controlled release influenced by time and pH. The cell study results revealed that Cur-PAMAM-MTX NC exhibited significantly higher cytotoxicity than free MTX, Cur, and other formulations tested in vitro. The synergistic effect of co-delivery of MTX and Cur by PAMAM significantly increased cytotoxicity. Besides, the significant ROS level rising has been shown in the treated cells with MTX-PAMAM-Cur. Considering these findings, the co-delivery NC shows promise for additional in vitro investigations and possesses the capacity to function as an effective framework for the combined delivery of MTX and Cur in cervical cancer chemotherapy.

Keywords Curcumin, PAMAM dendrimer, Methotrexate, Nanocomplex

In recent years, cervical cancer became a significant factor in the elevated number of deaths associated with cancer in women[1]. Insufficient information about the mechanism of action of many anticancer drugs and their side effects of their use often make the treatment fail. The drawbacks associated with cytotoxic chemotherapy have sparked a growing fascination with natural products and traditional herbal medicine, both in contemporary and ancient worlds[2,3]. Curcumin (Cur) is a naturally existing substance extracted from the turmeric rhizome, known for its varied therapeutic characteristics, such as anti-angiogenic, anti-inflammatory, and antitumor properties[4,5]. Numerous apoptotic signaling pathways, including signal transducer and activator of transcription 3 (STAT3), phosphoinositide 3-kinase/(PI3K)/Akt, and nuclear factor-kappaB (NF-κB) contribute to the potential anticancer characteristics of Cur. On the other hand, its cytotoxic effect on normal cells and tissues is low[6]. However, the practical application of Cur in clinical environments is constrained by its low solubility in

[1]Research Center for Pharmaceutical Nanotechnology, Tabriz University of Medical Sciences, Tabriz, Iran. [2]Department of Biology, Faculty of Basic Sciences, Azarbaijan Shahid Madani University, Tabriz, Iran. [3]Pharmaceutical Analysis Research Center, Tabriz University of Medical Sciences, Tabriz, Iran. [4]Drug Applied Research Center, Tabriz University of Medical Sciences, Tabriz, Iran. [5]Research Center for Food Hygiene and Safety, School of Public Health, Shahid Sadoughi University of Medical Sciences, Yazd, Iran. [6]Department of Food Hygiene and Safety, School of Public Health, Shahid Sadoughi University of Medical Sciences, Yazd, Iran. [7]Laser Research Centre, Faculty of Health Science, University of Johannesburg, Doornfontein 2028, South Africa. [8]Ayuob Aghanejad and Shiva Kheiriabad contributed equally to this work. ✉email: ezzatij@tbzmed.ac.ir; andishmand.hashem@gmail.com; hamblin@helix.mgh.harvard.edu

water and instability, resulting in reduced bioavailability within cancer cells[7]. Consequently, various approaches have been undertaken to enhance the therapeutic effectiveness of Cur[8,9]. Curcumin is frequently paired with chemotherapy medications in the management of diverse cancer types[6]. Additionally, Methotrexate (MTX), acting as a folic acid (FA) antagonist, is widely employed as an anticancer medication for different types of cancer, frequently in conjunction with additional medications[10].

Recently, the tendency to investigate co-delivery systems has increased. Co-delivery systems enable the efficient delivery of optimal doses of drug combinations or gene-drug mixtures, outperforming single-drug-loaded systems in terms of speed and efficacy[11]. On the contrary, the co-delivery of drugs can reduce unwanted drug toxicity, facilitate drug passage through biological barriers, refine targeting, and increase the depth of drug penetration in tumors[12]. Polyamidoamine (PAMAM) dendrimers are a group of precisely structured and intricately branched synthetic macromolecules known for their well-defined compositions. These dendrimers feature internal cavities with modifiable surface functional groups, allowing for the encapsulation of drugs or other payloads. The versatile nature of PAMAM facilitates the regulation of interactions between PAMAM and drugs. Notably, PAMAM nanosystems possess advantageous properties such as biocompatibility, appropriate biodegradability, spherical form, regulated drug release, water solubility, minimal binding to blood proteins, and lack of immunogenicity. These attributes make PAMAM dendrimers suitable vehicles to deliver genetic material and medicine[13]. The versatile attachment site for various therapeutic agents is facilitated by the surface functional groups of PAMAM dendrimers. Crucially, this conjugation does not compromise the spherical structure of PAMAM dendrimers when they are in a solution[13].

In other words, in this study, for the first time, a fourth-generation (G4) PAMAM dendrimer was employed to simultaneously deliver MTX and Cur to human cervical carcinoma (HeLa) cells. Curcumin was encapsulated within the cavities of the PAMAM dendrimer, while MTX was covalently conjugated to the dendrimer.

Materials and methods

Materials

The HeLa cells were acquired from the National Cell Bank of Iran. Generation 4 (PAMAM-G4) EDTA core PAMAM dendrimer, 2-(4-aminophenyl)-6 indolecarbamidine dihyformaldehyde (DAPI), methotrexate, 3-(4,5-dimethyl-thiazol-2-yl)-2,5-diphenyl-tetrazolium bromide (MTT), curcumin from turmeric rhizome, and trypsin were sourced from Sigma Aldrich Company (St. Louis, MO, USA). Fetal bovine serum (FBS), penicillin-streptomycin, Roswell Park Memorial Institute (RPMI) 1640, trypsin-EDTA solution, and phosphate-buffered saline (PBS) were acquired from Gibco Life Technologies (Paisley, UK). The AnnexinV-FITC/PI apoptosis kit was obtained from oncogene research products (San Diego, USA). Dimethyl sulfoxide (DMSO) was prepared from Merck Chemical Co. (Darmstadt, Germany).

Synthesis of PAMAM-MTX nanocomplex

The preparation of PAMAM-MTX NC was performed according to Khatri et al.[14] with some modifications. Briefly, MTX (1 mg) and PAMAM G4 (10% w/v in methanol, with a density of 0.791 g/mL at 25 °C) in the ratio of 10:1 were dissolved in 1 mL of DMSO. Subsequently, 5 mg N, N′-Dicyclohexylcarbodiimide (DCC) was added to the solution. The mixture was continuously stirred in complete darkness at 25 °C for a duration of 72 h to form MTX dendrimer conjugate through a reaction between the $-NH_2$ end groups of the dendrimer and the –COOH group of MTX. The mixture underwent purification by dialysis against DMSO for 24 h to eliminate free DCC and MTX.

Preparation of Cur-PAMAM-MTX Nanocomplex

To determine the optimal 1:1 ratio, various w/w ratios of PAMAM-MTX and Cur (from 8:1 to 1:1) were initially evaluated[15,16]. 1 mL of methanolic solution of Cur (1 mg/mL) was slowly added drop by drop to a mixture of 1 mL of methanolic solution of PAMAM/MTX (1 mg/mL) and 2 mL of PBS (0.05 M, pH 7.4). Then the mixing was performed by stirring at 250 rpm for 24 h. To eliminate any unbound Cur, the PAMAM-MTX and Cur mixture was subjected to centrifugation at 5000 rpm and 4 °C for 15 min. The non-complexed Cur, which was not soluble in PBS, formed a precipitate and was removed[2]. The collected precipitate of free Cur was dissolved in 1 mL of methanol and UV-vis spectroscopy was employed to determine its amount. The resulting supernatant was carefully collected and stored in a dark chamber at 4 °C for subsequent in vitro experimental assays[2].

Evaluation of drug loading

The %EE of curcumin was assessed, using Amicon centrifugal filter ((Millipore, MW cut off 100 kDa)[17]. The dispersion of Cur-PAMAM-MTX NC was placed on the upper compartment of Amicon® tubes and centrifuged at 4000 rpm for 30 min to separate free curcumin from the lower compartment of Amicon®. The amount of free curcumin was determined by using UV-vis spectrophotometry at a wavelength of 430 nm. The %EE were determined using Eq. 1.

$$\%\mathrm{EE} = \frac{\mathrm{A} - \mathrm{B}}{\mathrm{A}} \times 100 \quad (1)$$

A: Initial amount of Cur. B: Free Cur.

Characterization of Cur-PAMAM-MTX nanocomplex

FT-IR was employed to observe the potential interaction between MTX and PAMAM, facilitating the preparation of the PAMAM-MTX NC. In addition, the dynamic light scattering technique (Malvern Zetasizer Nano-ZS instrument) was used to evaluate the hydrodynamic size and zeta potential (ZP) of PAMAM dendrimer, PAMAM-MTX, Cur-PAMAM, and Cur-PAMAM-MTX nanocomplexes[18].

Particle morphology

The morphology of nanocarriers was determined applying atomic force microscopy (Flex-AFM, Nanosurf AG; Liestal, Switzerland). For AFM sample preparation, nanocarriers were diluted with water, with a dilution factor according to the technical requirement of AFM, and a droplet of 2 mL was placed onto a freshly cleaved mica substrate (1 cm^2) and was air-dried. AFM measurements were performed in intermittent contact mode.

Curcumin release from Cur-PAMAM-MTX nanocomplex

The release of Cur from the Cur-PAMAM-MTX NC was assessed using the dialysis bag technique under sink condition. To begin, the Cur-PAMAM-MTX NC, which included Cur at a concentration of 1 mg/mL, was dissolved in 5 mL of PBS. This solution was then placed inside a dialysis bag with a molecular weight cutoff (MWCO) of 12 kDa. The dialysis bags were subsequently immersed in 50 mL PBS solutions with different pH levels (5.4, 6.4, and 7.4) and kept at a temperature of 37 °C on a horizontal shaker set at 200 rpm. At specific time intervals, 2 mL samples were taken out, and an equal volume of fresh buffer solution was added. The cumulative release of Cur was monitored over a period of 48 h using UV-vis spectrophotometry at a wavelength of 430 nm[19–21].

Cell viability assay

The HeLa cancer cell lines, acquired from the national cell bank of Iran (Pasteur Institute, Tehran, Iran), were grown in RPMI-1640 medium supplemented with 10% FBS and antibiotics (50 unit/mL streptomycin and 100 unit/mL penicillin). The cells were placed in a culture medium and allowed to incubate in a controlled environment (95% humidity, temperature 37 °C, 5% CO_2) until reaching 70% confluence. Cytotoxicity effects of various formulations on cancer cells were evaluated utilizing the MTT assay. Initially, 1×10^4 cells were seeded in 96-well plates with 200 µL of culture media and incubated. After 24 h, different groups, including PAMAM-MTX, Cur-PAMAM, and Cur-PAMAM-MTX at concentrations in the range of 10 to 200 µM/mL in growth medium were introduced into each well and cells were incubated for 24 and 48 h. Subsequently, 50 µL of MTT solution (2 mg/mL) was introduced to each well. After a 4 h incubation, the medium was substituted with 200 µL of DMSO. Finally, absorbance measurements at a wavelength of 570 nm were assessed with a spectrophotometric plate reader (BioTek Instruments Inc, Vermont, USA)[22,23].

Apoptosis assay

For this analysis, HeLa cells were cultured in 6-well plates with a density of 2×10^5 cells per well. They were then placed in a complete cell culture medium and allowed to incubate until they achieved a confluence of more than 70%. Afterwards, the cells were treated with various formulations containing PAMAM, Cur, MTX, Cur-PAMAM, PAMAM-MTX, and Cur-PAMAM-MTX and incubated for 48 h. After the incubation period, the cells were collected and separated by the addition of diluted trypsin, washed three times in PBS, and re-suspended in binding buffer. To determine the rate of cell apoptosis, the cells were detached and stained using the Annexin V/PI kit. The resulting data were then analyzed by the FlowJo software (version 7.0)[23,24].

DAPI staining

DAPI staining was employed to detect apoptotic cells according to Bakhtiary et al.[25] with some modifications. Initially, cells (2×10^5 per well) were trypsinized and cultured in 6-well plates. Once reaching sufficient confluency (70%), the cells were subjected to different treatments including PAMAM, Cur, MTX, Cur-PAMAM, PAMAM-MTX, and Cur-PAMAM-MTX, subsequently, a period of 48 h followed. After the 48 h treatment period, the cells were washed with PBS three times. Subsequently, they were fixed with paraformaldehyde (4%) for 2 h and incubated with Triton X-100 solution (1%) for 5 min. The treated cells were then stained using 50 µL of DAPI solution. Finally, DNA fragmentation was visualized using a Cell Imaging Multi-Mode Reader (BioTekCytation™ 5, USA)[25].

Reactive oxygen species (ROS) assessment

Intracellular ROS levels has been evaluated using Dichlorodihydrofluorescein diacetate (DCFH-DA). Briefly, cells were seeded on a 6-well Cell Culture Slides plate (1×10^4 cells/well). After cell attachment, they were treated and incubated with 25 µM DCFH-DA solution (ab113851) for 45 min at 37 °C. Then, 1X PBS buffer was used for the stained cells washing and the nuclei were stained with DAPI for 5 min. Finally, fluorescence signal of DCF and DAPI at Ex/Em: 485/535 nm and 358 /461 was identified by fluorescence microscope (Olympus BX50), respectively[26].

Statistical analysis

Statistical analysis of the data was done using Graph Pad Prism 6.0 software (https://www.graphpad.com/demos/) and a two-way analysis of variance (ANOVA). Statistical significance was determined with a P-value < 0.05. All experiment were conducted three times for reliability and the results were expressed as mean ± standard deviation (SD).

Results

Confirmation of PAMAM-MTX nanocomplex synthesis

FT-IR spectroscopy was utilized to evaluate the possible interaction between PAMAM dendrimers and MTX. The absorption peaks of MTX showed O-H and N-H bands at 3373 cm^{-1}, 3362 cm^{-1} and 3201 cm^{-1} and C = O, carbonyl amide and C-N band at 1639 cm^{-1}, 1607 cm^{-1} and 1566 cm^{-1} respectively. Also, the absorption peaks of PAMAM exhibited N-H and $-NH_2$, carbonyl amide and C-N bands at 3400 cm^{-1}, 3261 cm^{-1}, 1649 cm^{-1}, and 1554 cm^{-1}, respectively. Based on the FT-IR findings, the absorption peaks of PAMAM-MTX related to O-H and N-H was showen at 3436 cm^{-1} and the decrease in the absorption peaks of O-H and C = O at 3373 cm^{-1}, and 1639 cm^{-1}, respectively was seen. In addition, formation of amide band between carboxylic group of MTX and amine groups of PAMAM at 1652 cm^{-1} is demonstrative of MTX conjugation in PAMAM dendrimers. (Fig. 1)[14].

Fabrication of Cur loaded PAMAM-MTX nanocomplex

The results revealed distinct absorption spectra for Cur, PAMAM, and the Cur-loaded PAMAM-MTX system. In particular, the absorbance curves of Cur alone and Cur-PAMAM were distinguished by a significant peak at 430 nm and a smaller peak around 370 nm. The incorporation of Cur into the pockets of PAMAM led to an improved absorption of Cur, causing a shift towards longer wavelengths compared to Cur alone at a similar concentration. The %EE of the Cur-PAMAM-MTX NC were around ~81%. This can be attributed to the selection of a 1:1 (w/w) ratio between PAMAM dendrimer and Cur[26].

Characterization of nanocomplex size and zeta potential

The results of particle size and ZP of NPs (Table 1) indicated an increase in hydrodynamic sizes for Cur-PAMAM-MTX NC compared to PAMAM dendrimer alone, complemented by a reduction in the ZP value (Table 1). The mean particle sizes were measured as 3.94, 2.71, 110.50 ± 2.54, and 249.12 ± 15.04 nm, with ZP of 6.93, 7.80, 2.69, and −3.28 mV for PAMAM, Cur-PAMAM, MTX-PAMAM, and Cur-PAMAM-MTX NC, respectively. Notably, the Cur-PAMAM-MTX NC exhibited a relatively narrow polydispersity index (PDI) = 0.374. This indicates a more uniform size distribution and favorable properties for drug delivery[27]. In addition, the results obtained from AFM images showed the average size of 95.91 ± 2.00 and 197.51 ± 4.05 for PAMAM-MTX and Cur-PAMAM-MTX NC, respectively that are in accordance with dynamic light scattering results (Fig. 2). Also, the SEM images of PAMAM, PAMAM-Cur, PAMAM/MTX, and PAMAM-Cur-MTX have been demonstrated in Fig. 3.

Cur Release Profile

The in vitro release of Cur from the Cur-PAMAM complex in PBS with pH values of 7.4, 6.4, and 5.4 over a period of 48 h was evaluated using the dialysis method compared to free Cur. This approach simulated the release of Cur under both physiological conditions and in an acidic tumor environment. As depicted in Fig. 4, a substantial release of Cur from the Cur-PAMAM-MTX complex occurred at pH 5.4 within the initial 10 h, with a release of approximately 40%. It is worth mentioning that during the 48 h duration, the release of Cur from Cur-PAMAM-MTX complex at pH 5.4 was approximately 50%, while the release decreased to 30% at pH 6.4 and 15% at physiological pH (7.4) but in the same condition release values for free Cur were 100, 80 and 60% at pH 5.4, 6.4 and 7.4, respectively after 48 h[28].

Cell viability assay

This experiment was applied to evaluate the synergistic effects of dual drugs and the enhanced benefits when they were loaded into PAMAM. First, the cytotoxicity of the Cur, MTX, and their combination (MTX/Cur) on Hela cancer cells was assessed by the MTT assay. According to Fig. 5A, IC_{50} of the Cur/MTX was around 10 µM/mL in 24 h which reduced to almost 5 µM/mL after 48 h. Then the cytotoxicity of Cur-PAMAM, PAMAM-MTX, and Cur-PAMAM-MTX NC on HeLa cancer cells within the concentration range of 10–200 µM/mL was assessed in 24 h and 48 h. The results, depicted in Fig. 5, indicated a time- and concentration-dependent prohibition of cell progression for all treatment groups after both 24 and 48 h. Notably, Cur-PAMAM-MTX NC Showed the least cell viability in comparison to the other formulations. After 24 h, the IC_{50} values obtained from the MTT assay for Cur-PAMAM and Cur-PAMAM-MTX NC were 40 and 35 µM/mL, respectively, and after 48 h, they reached 20 and 12 µM/mL. Additionally, the IC_{50} value for PAMAM-MTX on HeLa cells was 190 and 35 µM/mL after 24 and 48 h, respectively. Furthermore, the findings demonstrated that the PAMAM dendrimer, when not loaded with Cur or MTX, did not exhibit any decrease in cell viability, even at elevated concentrations in HeLa cell lines (data not shown).

Annexin V-FITC apoptosis assay

To evaluate cell apoptosis in different treatment groups, Annexin V-FITC/PI staining was performed on HeLa cancer cells. Initially, HeLa cells were exposed to different treatment groups, including free Cur, MTX, PAMAM dendrimer alone, Cur-PAMAM, PAMAM-MTX, and Cur-PAMAM-MTX NC, for 48 h. Subsequently, flow cytometry was utilized to determine the proportion of cells in the early apoptotic (Annexin V+/PI-), late apoptotic (Annexin V+/PI+), living (Annexin V-/PI-), and necrotic cells (Annexin V+/PI+). As illustrated in Fig. 6, the proportions of cells undergoing apoptosis in the PAMAM, free Cur, MTX, Cur-PAMAM, PAMAM-MTX, and Cur-PAMAM-MTX NC groups were 0.07%, 71.3%, 1.62%, 70.01%, 0.96%, and 77.9%, respectively. According to Fig. 7, in the various treatment groups, the highest percentage of apoptosis was observed in the Cur-PAMAM-MTX NC group. Conversely, no significant apoptosis was detected in the cells treated with PAMAM-MTX and MTX. Additionally, the PAMAM dendrimer alone exhibited the lowest proportion of apoptosis among the treated groups, indicating its safety in drug delivery.

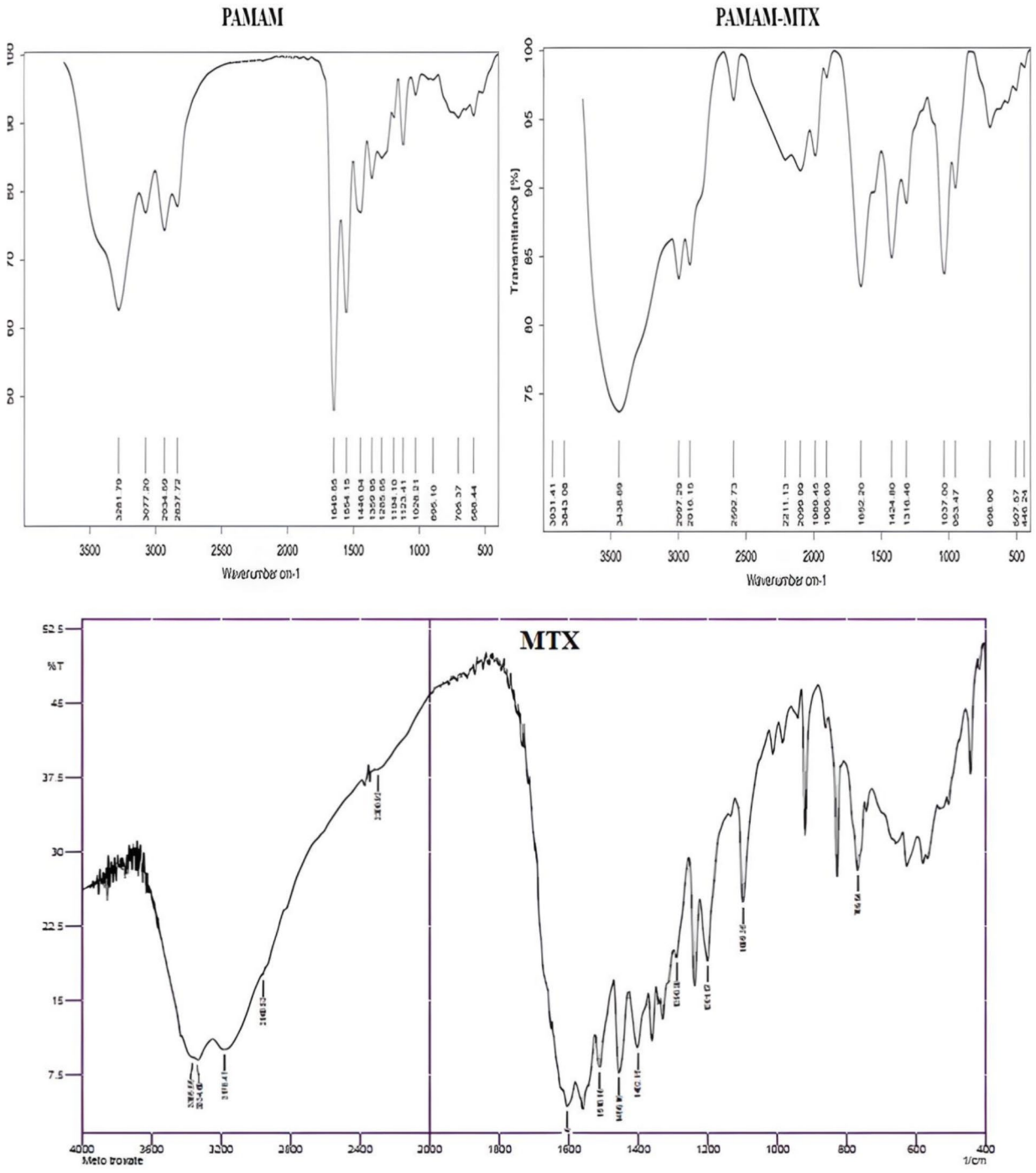

Fig. 1. FTIR spectra of blank PAMAM, MTX, and PAMAM/MTX.

DAPI staining analysis

The DAPI staining test was done to evaluate the existence of fragmented and condensed DNA in cells undergoing apoptosis. Figure 6 displays microscopic snapshots of HeLa cells stained with DAPI following a 48 h exposure to the IC_{50} concentration of PAMAM dendrimer alone, free Cur, MTX alone, Cur-PAMAM, PAMAM-MTX, Cur-PAMAM-MTX NC, and cells left untreated (negative control). Predominantly, typical morphological changes indicative of apoptosis was observed in all treated groups, including Cur, MTX, Cur-PAMAM, PAMAM-MTX, and Cur-PAMAM-MTX NC (Fig. 6). In contrast, untreated cells and PAMAM dendrimer alone did not exhibit any alterations in cell morphology. Moreover, both PAMAM-MTX and MTX alone exhibited slight signs of apoptotic cell features. As illustrated in Fig. 7, the DAPI staining results indicated that the concurrent administration of MTX and Cur using PAMAM dendrimer resulted in the most pronounced

Samples	Size ± SD (nm)	ζ potential ± SD (mv)	PDI
PAMAM-Cur-MTX	249.12 ± 15.04	-3.28 ± 0.157	0.374
PAMAM/MTX	110.50 ± 2.54	2.69 ± 0.270	0.206
PAMAM-Cur	2.71 ± 0.75	7.80 ± 0.920	1
PAMAM	3.94 ± 0.87	6.93 ± 0.538	0.5

Table 1. Particle size and zeta potential of PAMAM, PAMAM-Cur, PAMAM/MTX and PAMAM-Cur/MTX ($n = 3$).

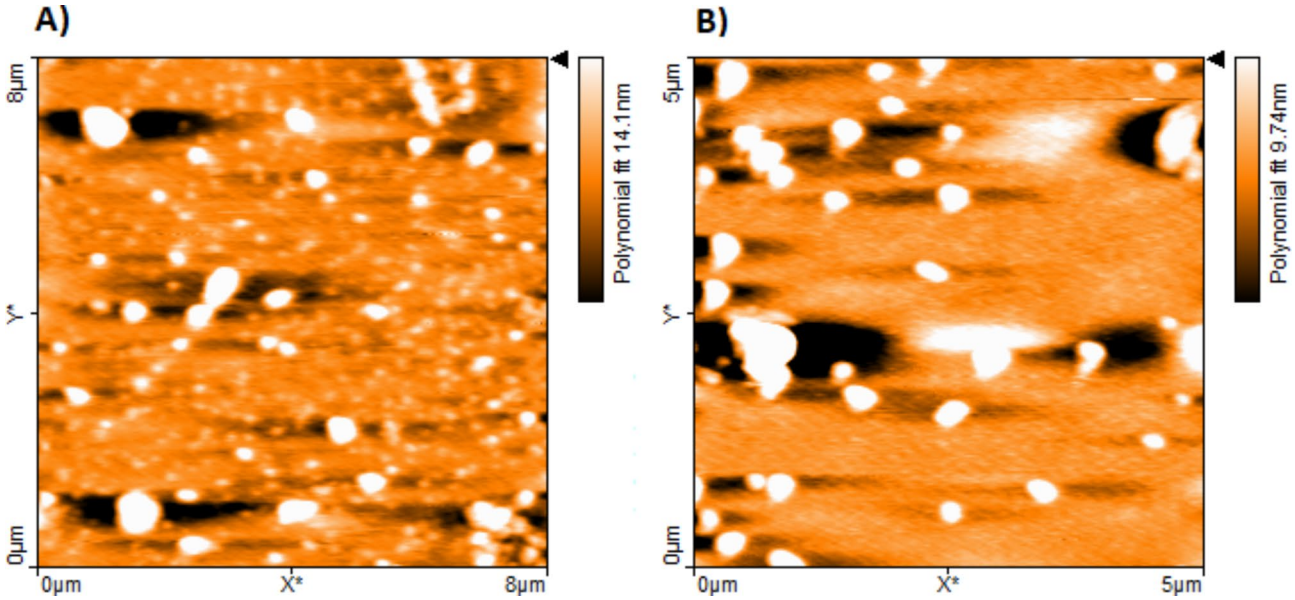

Fig. 2. Atomic force microscopy images of PAMAM/MTX (A), and PAMAM-Cur/MTX (B).

nuclear condensation and chromatin fragmentation (common indicators of cell apoptosis) in HeLa cells after 48 h, which was consistent with the findings from Annexin V-FITC/PI staining.

Assessment of ROS

DCFH-DA undergoes hydrolyzation by intracellular esterases to nonfluorescent DCFH as soon as entering the cytoplasm and DCFH oxidization led to the formation of fluorescent 2`, 7`-dichlorofluorescine (DCF) in the presence of ROS. As shown in Fig. 8, the untreated cells had been not shown any symptom of ROS existence, while treated cells with IC50 concentration of PAMAM, Cur, MTX, PAMAM-MTX and MTX-PAMAM-Cur indicated ROS level rising and the most noteworthy increase in ROS level has been observed in the cells treated with MTX-PAMAM-Cur.

Discussion

Apoptosis is a crucial factor in the treatment of cervical cancer. Irregularities in the usual function of apoptotic signaling pathways play a role in the onset of malignancies and the progress of resistance to conventional chemotherapy medications[2]. MTX and Cur were chosen based on their distinctive biological and physicochemical characteristics. Curcumin possesses the capacity to impact diverse cell signaling pathways, showcasing a multifaceted therapeutic impact in cancer treatment. However, its application as a chemotherapeutic agent is constrained by challenges such as limited solubility in water, instability, and inadequate bioavailability[29–31]. Furthermore, it is widely recognized that Cur can enhance the anticancer efficacy of various medicines such as doxorubicin and paclitaxel. It enhances the absorption and cytotoxic effects of MTX in KG-1 leukemic cells[32]. MTX, an antimetabolite with structural similarity to FA, disrupts the synthesis of RNA and DNA by obstructing DHFR, a pivotal enzyme in the folate cycle. This ultimately results in cellular apoptosis[32]. PAMAM dendrimers, widely recognized as highly efficient nanocarriers in biological studies, have the potential to accumulate in tumor tissues as a result of their nanoscale dimensions, promoting the enhanced permeability and retention (EPR) effect[2,33]. In this study, we propose an approach wherein Cur is encapsulated within the hydrophobic compartment, while MTX is conjugated onto the hydrophilic surface of PAMAM nanocarriers. This strategy is suggested to improve the antitumor effectiveness of the formulation. The loading of Cur into the nanocarrier was achieved, and the encapsulation of the drug was quantified using UV-Vis spectrophotometry after a dialysis step, representing the time required to purify nanocomplexes from unencapsulated Cur. A high% EE value of 81%

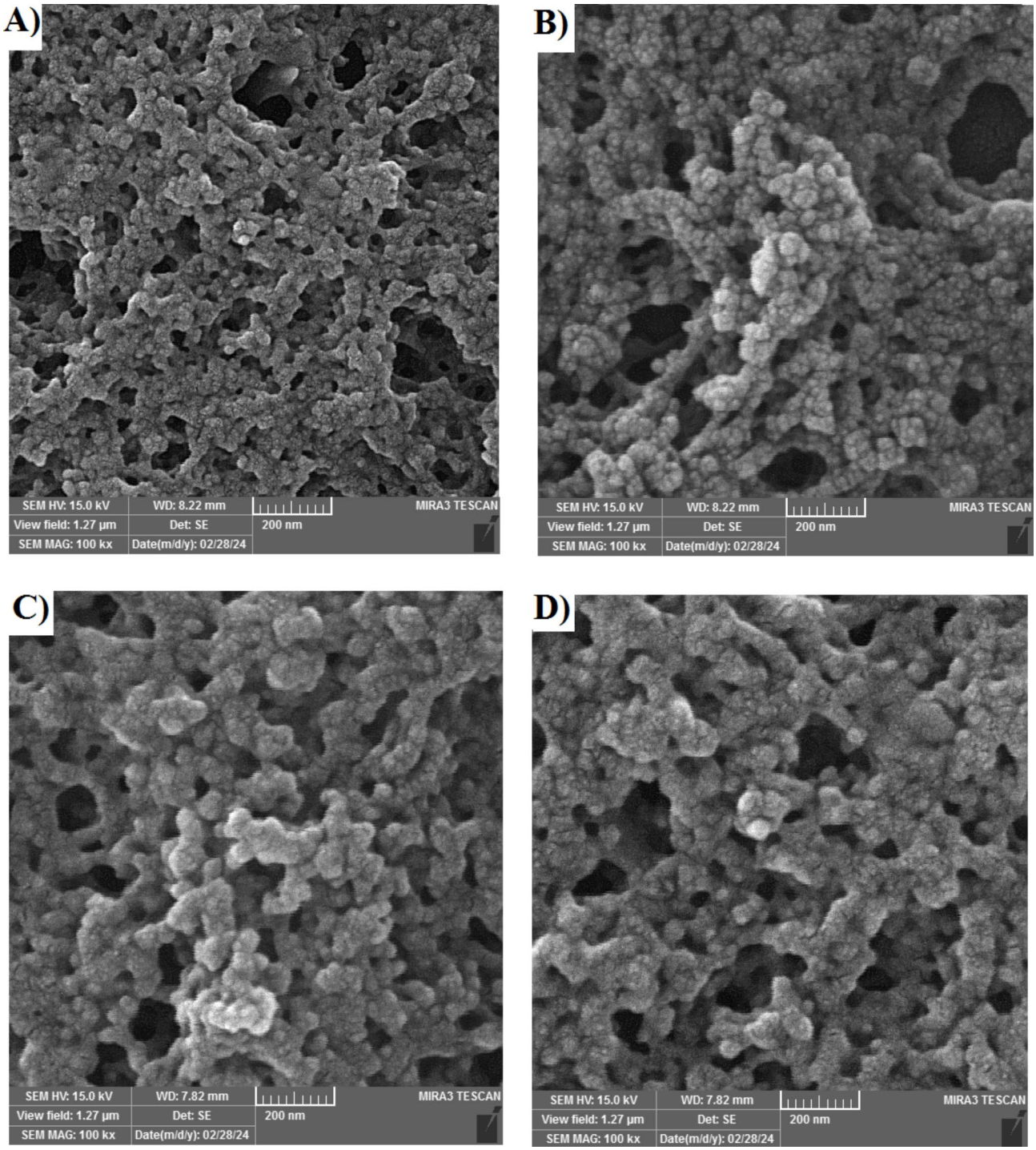

Fig. 3. SEM images of (**A**) PAMAM, (**B**) PAMAM-Cur, (**C**) PAMAM/MTX, (**D**) PAMAM-Cur-MTX.

was observed for Cur, indicating substantial drug encapsulation within the NPs. Following that, experiments for drug release were performed at pH of 5.4, 6.4, and 7.4[32]. Cur-PAMAM-MTX NC exhibited an average diameter 249.12 ± 15.04 nm, which was higher than the dimensions (> 50 nm) to be accumulated in the liver.

Hence, our formulations are anticipated to access tumor vasculature through the EPR effect as described by Maeda[34]. A PDI value < 0.5 signifies a particle size distribution that is both narrow and homogeneous[35]. Consequently, the PDIs for PAMAM-MTX and PAMAM NC fell within the satisfactory range (0.3 and 0.5). Cur-PAMAM and Cur-PAMAM-MTX NC exhibited PDIs of 1.0 and 0.374, respectively. Additionally, ZP serves as an indicator of NC stability. Having two distinct drugs in the NC seemed to decrease the ZP and, consequently, diminish its induced stability[36]. The ZP, indicating electrophoretic mobility, seems to be affected by both formulation and process parameters. In this study, it was noted that PAMAM NC and PAMAM NC loaded

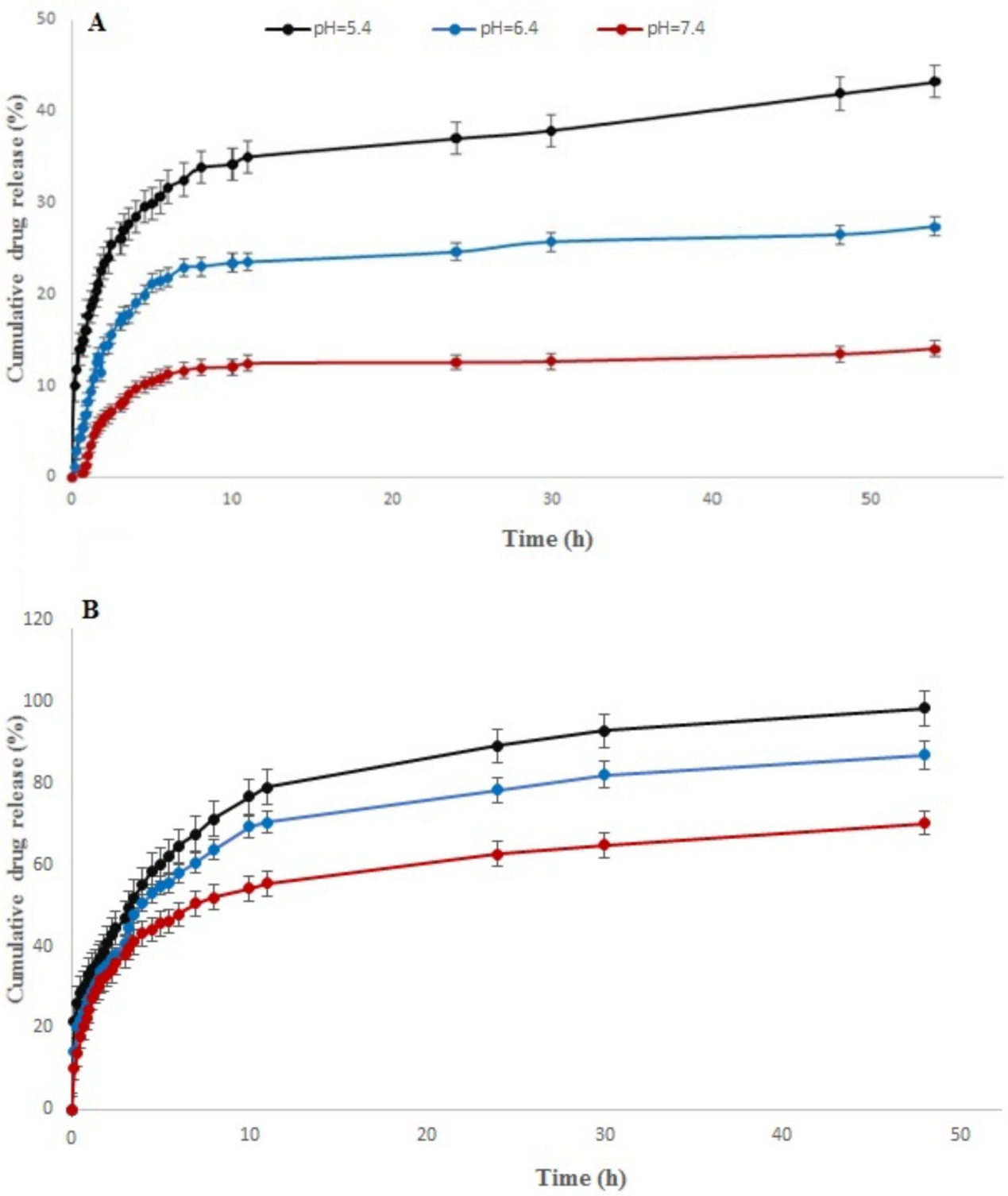

Fig. 4. (A) In vitro Cur release profiles of PAMAM-Cur/MTX in PBS (pH 7.4, pH 5.4, pH 6.4) at 37 °C. (B) In vitro release profiles of free Cur at the same condition.

with Cur exhibited similar ZP ranging from 6.93 to 7.80 mV. This observation implies that Cur, likely owing to its hydrophobic characteristics, is fully enclosed within the polymer matrix. Additionally, Cur-PAMAM-MTX NC and PAMAM-MTX NC displayed lower ZP (-3.28, 2.69 mV, respectively) compared to the blank PAMAM NC. This decrease in ZP is likely related to the conjugation of MTX on the surface of NC[34].

The prepared formulations did not show any significant differences (p-value > 0.05) in terms of their ZP and PDI[36]. Syed et al.[37] co-encapsulated MTX and Cur by bovine serum albumin (BSA) NPS to maximize therapeutic

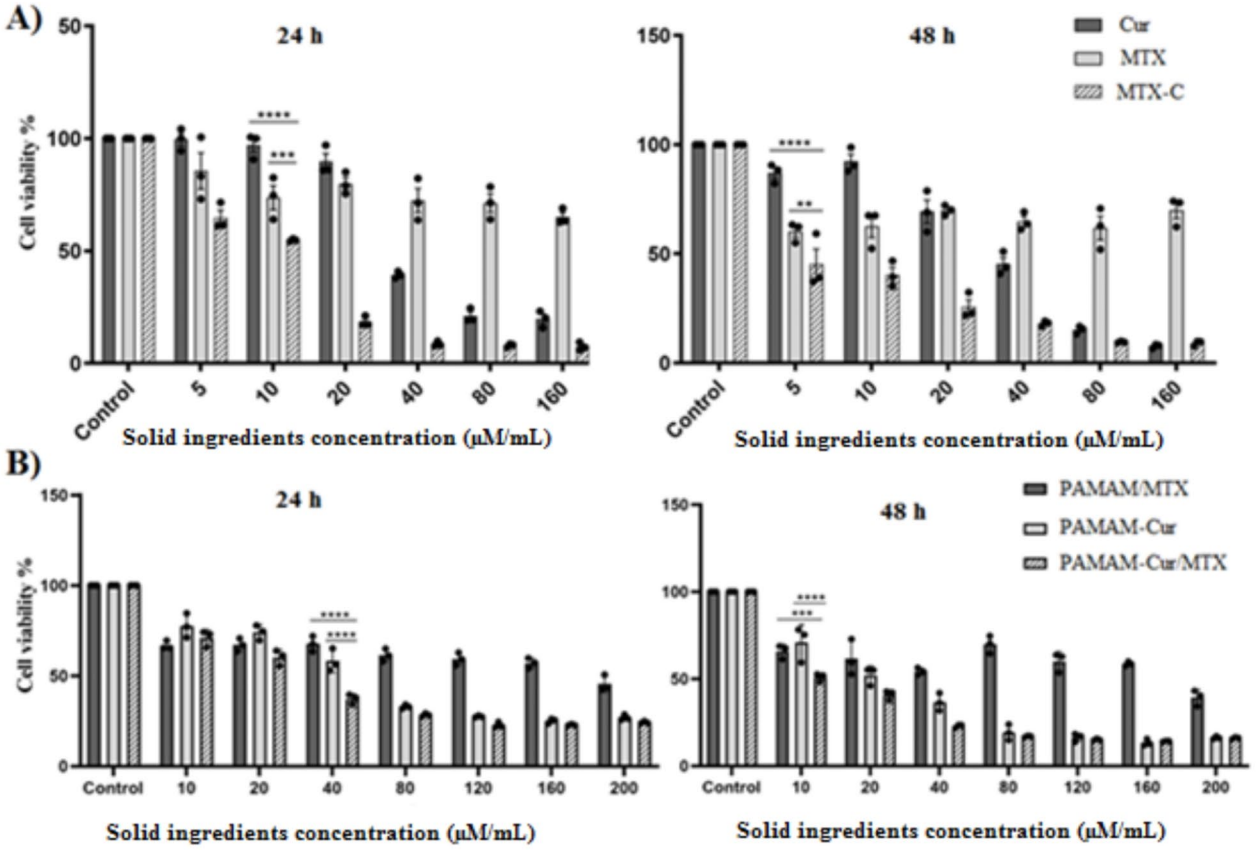

Fig. 5. (**A**) In vitro cytotoxicity of Cur, MTX and their combination, and (**B**) PAMAM-Cur, PAMAM/MTX, and PAMAM-Cur/MTX on HeLa cancer cells for 24 and 48 h. *$P < 0.05$, ** $P < 0.01$ and *** $p < 0.001$. Untreated cells are considered as a negative control ($n = 3$).

efficacy and reduce MTX-related toxic side effects and evaluated its structural properties. The particle size and PDI of prepared NPs were reported as 163.05 ± 1.708 nm and 0.195 ± 0.0024, respectively. NP_S was spherical in shape and also the release pattern of both MTX and Cur was gradual with %EE of 68.23 ± 0.640% for MTX and 75.71 ± 0.216% for Cur.

The time-dependent pattern and the degree of drug release offer crucial insights into the anticipated concentrations of the drug in vivo. In our findings, we noted an initial rapid release of Cur in formulations. Subsequently, Cur displayed a gradual release pattern like drugs encapsulated within a polymer matrix. This same release behavior for Cur has been demonstrated by Ghaffari et al.[2]. Our hypothesis suggests that the release of the encapsulated drug (Cur) can be attributed to the entrapment of Cur within the polymer matrix, causing a delay in drug release over the examined duration. Otherwise, the significant hydrophobic nature of Cur may also play a role in hindering the drug's movement towards the aqueous phase[34]. Furthermore, within the acidic pH environment of tumor cells, the internal tertiary amine groups of the dendrimer undergo protonation. This protonation induces an "extended conformation" of the dendrimer, causing diffusion, charge repulsion, and the release of Cur from the expanded noncomplex. This process facilitates the release of Cur into the cytosol through the proton sponge effect[8]. On the contrary, the dendrimer experiences contraction, constraining its swelling and resulting in dendrimer collapse at alkaline pH due to the deprotonation of tertiary amines. This deprotonation hinders the effective release of Cur from the NPs. Consequently, our results demonstrate a significant association between the pH value and the release rate of Cur from the PAMAM-Cur formulation[2]. Danaf ar et al.[38] fabricated polymeric NPs based on mPEG and Poly caprolactone (PCL) for co-encapsulation of MTX and Cur and evaluation of its toxic influence on MCF7. The results showed that mPEG-PCL-MTX-CUR had spherical structure and the rate of drug release from NPs in a lower pH environment was more than its release in a neutral environment.

HeLa cancer cells served as the testing ground to assess the efficacy of PAMAM NC as carriers for Cur and MTX. The Cur-PAMAM and PAMAM-MTX NCs demonstrated notable effectiveness in decreasing the viability of HeLa cancer cells. The antitumor efficiency was significantly improved by encapsulating the drugs into the nanosystem and attaching them to the nanocarriers surface in contrast to the unbound drug. This enhancement can be attributed to PAMAM dendrimers facilitating drug penetration into cells through endocytic processes[39]. This indicates that the more acidic environment of HeLa cells may more efficiently initiate drug release in the

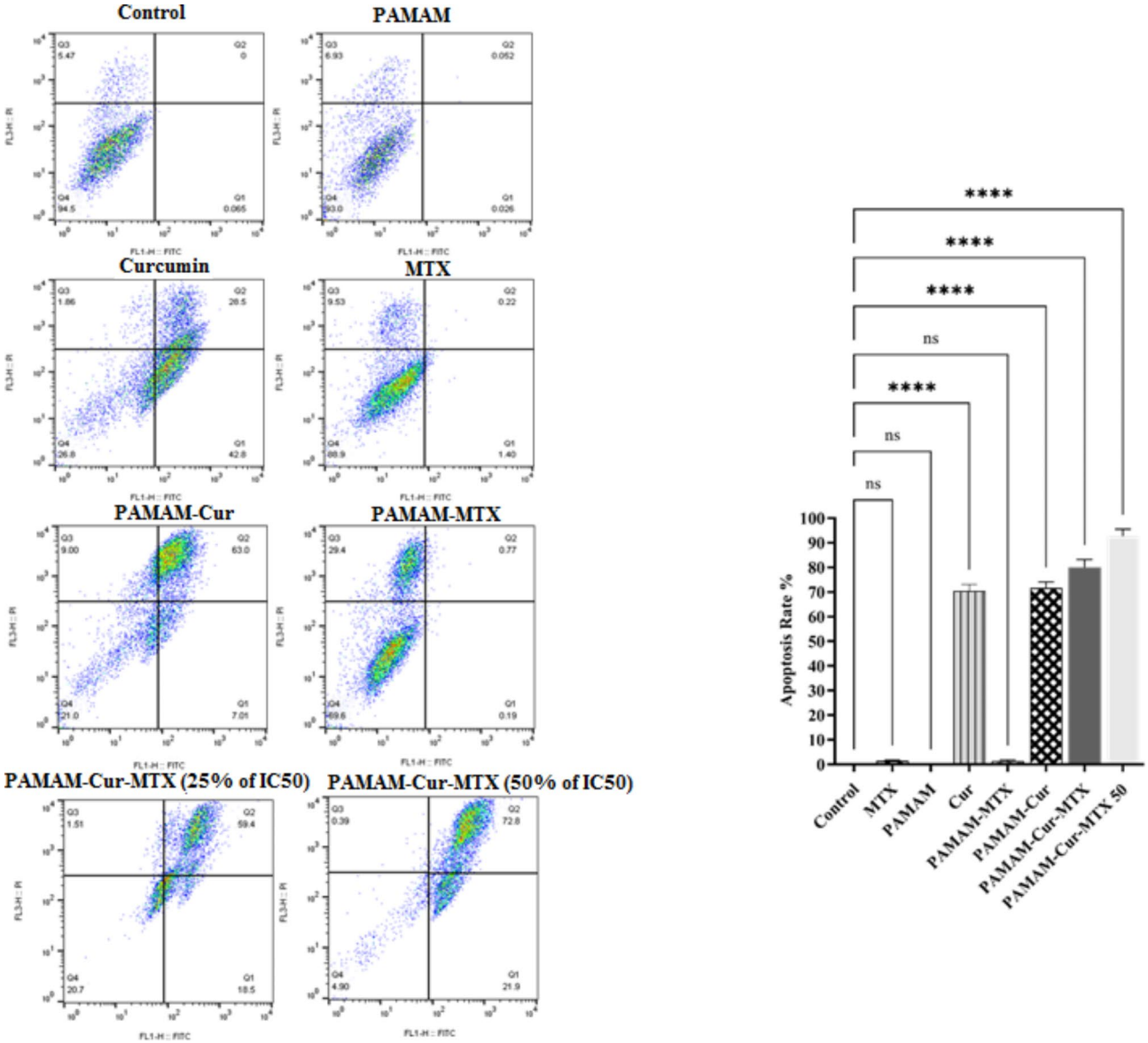

Fig. 6. Apoptosis histograms with apoptosis percentage of HeLa cancer cells analyzed by flow cytometry via AnnexinV/PI after 48 h incubation with free Cur, blank PAMAM, PAMAM-Cur, PAMAM/MTX, and PAMAM-Cur/MTX. *$P<0.05$, ** $P<0.01$ and *** $p<0.001$. Untreated cells were used as a negative control ($n=3$).

tumor cells. The Cur-PAMAM-MTX NC exhibited greater cytotoxicity compared to Cur-PAMAM alone. This proposes that the amalgamation of Cur-PAMAM with MTX yields a more powerful anticancer effect, especially in activating apoptotic signaling pathways[2]. These findings were consistent with the results of Mouszadeh et al.[40] who co-encapsulated Cur and MTX in a niosomal delivery system. The results of this study showed that by mixing CUR and MTX in niosomal formulation, higher apoptosis induction and greater prevention of cell migration can be achieved compared to mixing CUR and MTX in free form.

Moreover, the heightened cytotoxicity observed in the Cur-NC formulation can be attributed to the improved solubility and stability of Cur within PAMAM NCs, leading to enhanced Cur uptake through passive diffusion[26]. Moreover, a DAPI staining assay was employed to assess nuclear morphological changes, affirming that the Cur-PAMAM-MTX NC outperformed in inducing apoptosis in the treated HeLa cells[2]. While in vivo validation is crucial, the aforementioned findings indicated the potential utility of Cur-PAMAM-MTX NC for delivering two anticancer agents[10].

Conclusion

In summary, the newly developed Cur-PAMAM-MTX nanosystem proves to be an effective carrier for simultaneously delivering MTX and Cur in anticancer therapy. This research involved the successful preparation, optimization, and assessment of the Cur-PAMAM-MTX nanosystem for the co-delivery of MTX and Cur

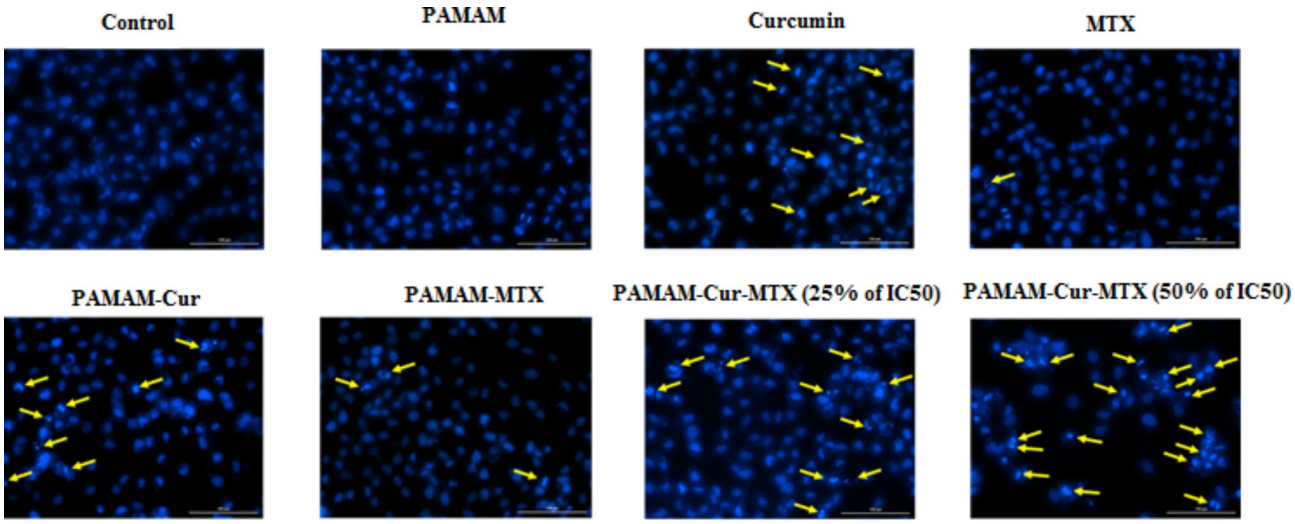

Fig. 7. Fluorescence microscopy images of HeLa cells stained with DAPI. The arrows show DNA and chromatin fragmentation with free Cur, PAMAM-Cur, PAMAM/MTX, and PAMAM-Cur/MTX.

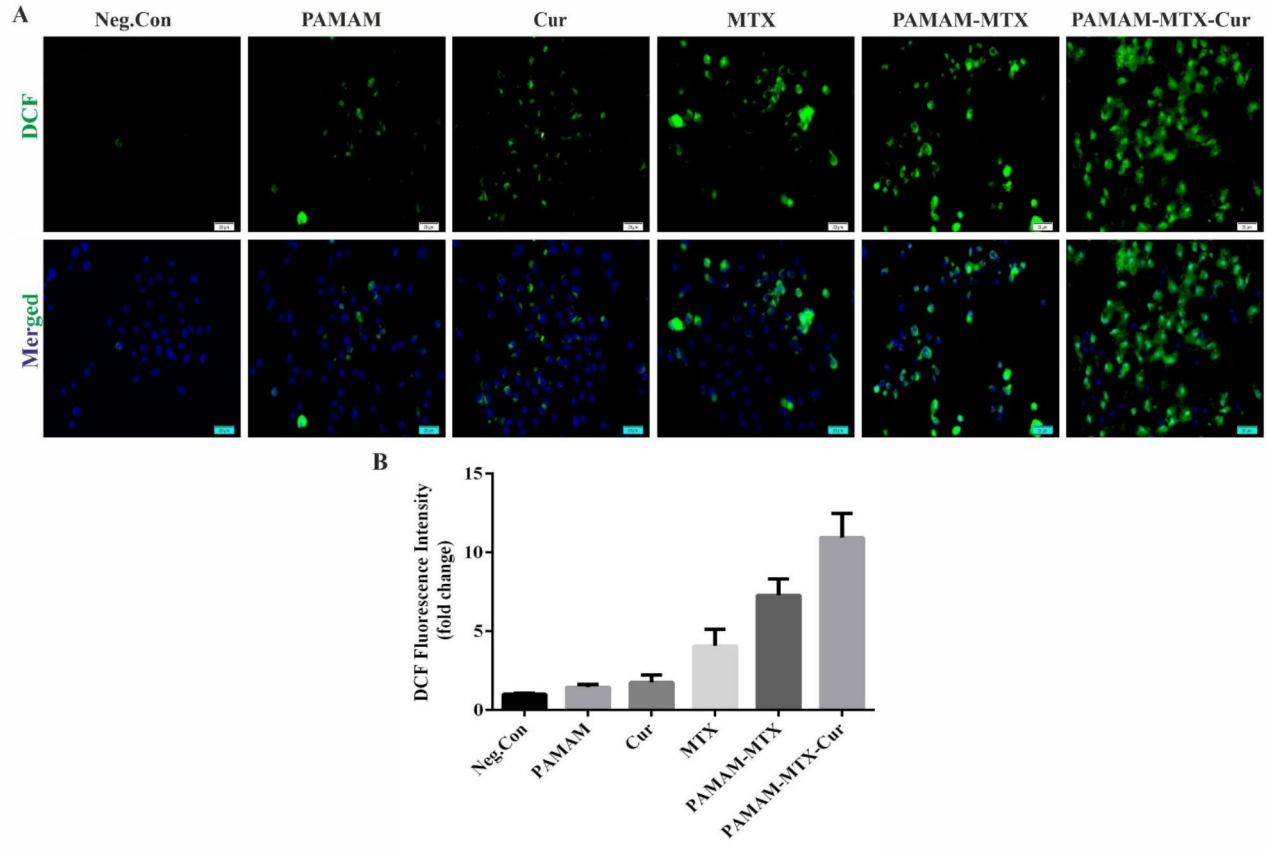

Fig. 8. Fluorescence microscopy images of HeLa cells treated with IC50 concentrations of various groups for evaluation of ROS level (A) Negative control group, (B) PAMAM, (C) Cur, (D) MTX, (E) MTX-PAMAM, (F) MTX-PAMAM-Cur.

to human cervical cancer (HeLa) cells. The resulting Cur-PAMAM-MTX NCs exhibited favorable in vitro characteristics and high cytotoxicity on the HeLa cell line. The present study revealed that Cur-PAMAM-MTX NC induced higher apoptosis in HeLa cells compared to other formulations and free drugs, indicating their potential as a candidate for synergistic co-delivery of antitumor agents for cervical cancer treatment. Also, the

most significant ROS generation has been seen in the cells treated with MTX-PAMAM-Cur nanosystem. The observed efficacy of the Cur-PAMAM-MTX nanosystem suggests that it has the potential to be used as an efficient strategy for cervical cancer chemotherapy. Nevertheless, despite these encouraging results, it is crucial to carry out additional in vivo investigations to confirm the viability of these systems in real-world applications. Also, more studies should be done to show synergism of both involved drugs.

Data availability

The datasets used and/or analysed during the current study available from the corresponding author on reasonable request.

Received: 3 May 2024; Accepted: 2 December 2024
Published online: 13 January 2025

References

1. Cohen, P. A. et al. Cervical cancer. *Lancet* **393** (10167), 169–182 (2019).
2. Ghaffari, M. et al. Co-delivery of curcumin and Bcl-2 siRNA by PAMAM dendrimers for enhancement of the therapeutic efficacy in HeLa cancer cells. *Colloids Surf., B.* **188**, 110762 (2020).
3. Gheybalizadeh, H. et al. Functionalizing of magnetic nanoparticles as nano-architecture towards bioimaging and colorimetric recognition of MCF-7 cells: dual opto-sensing and fluorescence monitoring for early-stage diagnosis of breast cancer. *Microchim. Acta* **191**, 752 (2024).
4. Zhang, J. et al. Self-carried curcumin nanoparticles for in vitro and in vivo cancer therapy with real-time monitoring of drug release. *Nanoscale* **7** (32), 13503–13510 (2015).
5. Revathy, S., Elumalai, S. & Antony, M. B. Isolation, purification and identification of curcuminoids from turmeric (Curcuma longa L.) by column chromatography. *J. Exp. Sci.* **2**(7) (2011).
6. Ni, W. et al. Dual-targeting nanoparticles: Codelivery of curcumin and 5-fluorouracil for synergistic treatment of hepatocarcinoma. *J. Pharm. Sci.* **108** (3), 1284–1295 (2019).
7. Ahmad, I. et al. Curcumin, its derivatives, and their nanoformulations: Revolutionizing cancer treatment. *Cell Biochem. Funct.* **42** (1), e3911 (2024).
8. Suo, A. et al. Folate-decorated PEGylated triblock copolymer as a pH/reduction dual-responsive nanovehicle for targeted intracellular co-delivery of doxorubicin and Bcl-2 siRNA. *Mater. Sci. Engineering: C.* **76**, 659–672 (2017).
9. Feng, T. et al. Liposomal curcumin and its application in cancer. *Int. J. Nanomed.* **12**, 6027 (2017).
10. Ashwanikumar, N. et al. Dual drug delivery of 5-fluorouracil (5-FU) and methotrexate (MTX) through random copolymeric nanomicelles of PLGA and polyethylenimine demonstrating enhanced cell uptake and cytotoxicity. *Colloids Surf., B.* **122**, 520–528 (2014).
11. Li, Q. et al. Mitochondrial membrane potential played crucial roles in the accumulation of berberine in HepG2 cells. *Biosci. Rep.* **39** (4), BSR20190477 (2019).
12. Majidzadeh, H. et al. Nano-based delivery systems for berberine: A modern anti-cancer herbal medicine. *Colloids Surf., B.* **194**, 111188 (2020).
13. Ghaffari, M. et al. Surface functionalized dendrimers as controlled-release delivery nanosystems for tumor targeting. *Eur. J. Pharm. Sci.* **122**, 311–330 (2018).
14. Khatri, S., Das, N. G. & Das, S. K. Effect of methotrexate conjugated PAMAM dendrimers on the viability of MES-SA uterine cancer cells. *J. Pharm. Bioallied Sci.* **6** (4), 297 (2014).
15. Farhangi, B. et al. Protective effects of dendrosomal curcumin on an animal metastatic breast tumor. *Eur. J. Pharmacol.* **758**, 188–196 (2015).
16. Babaei, E. et al. Dendrosomal curcumin significantly suppresses cancer cell proliferation in vitro and in vivo. *Int. Immunopharmacol.* **12** (1), 226–234 (2012).
17. Simion, V. et al. Development of curcumin-loaded poly (hydroxybutyrate-co-hydroxyvalerate) nanoparticles as anti-inflammatory carriers to human-activated endothelial cells. *J. Nanopart. Res.* **15**, 1–15 (2013).
18. Medel, S. et al. Curcumin-bortezomib loaded polymeric nanoparticles for synergistic cancer therapy. *Eur. Polymer J.* **93**, 116–131 (2017).
19. Li, C., Ge, X. & Wang, L. Construction and comparison of different nanocarriers for co-delivery of cisplatin and curcumin: A synergistic combination nanotherapy for cervical cancer. *Biomed. Pharmacother.* **86**, 628–636 (2017).
20. Kumari, P. et al. Transferrin-anchored poly (lactide) based micelles to improve anticancer activity of curcumin in hepatic and cervical cancer cell monolayers and 3D spheroids. *Int. J. Biol. Macromol.* **116**, 1196–1213 (2018).
21. Kesharwani, P. et al. Hyaluronic acid-conjugated polyamidoamine dendrimers for targeted delivery of 3, 4-difluorobenzylidene curcumin to CD44 overexpressing pancreatic cancer cells. *Colloids Surf., B.* **136**, 413–423 (2015).
22. Dolatabadi, J. E. N. et al. Formulation, characterization and cytotoxicity evaluation of ketotifen-loaded nanostructured lipid carriers. *J. Drug Deliv. Sci. Technol.* **46**, 268–273 (2018).
23. Mohammadzadeh-Aghdash, H. et al. Safety assessment of sodium acetate, sodium diacetate and potassium sorbate food additives. *Food Chem.* **257**, 211–215 (2018).
24. Yu, S. et al. *Galangin (GG) Combined with Cisplatin (DDP) to Suppress Human lung cancer by Inhibition of STAT3-regulated NF-κB and Bcl-2/Bax Signaling Pathways*97p. 213–224 (Biomedicine & Pharmacotherapy, 2018).
25. Bakhtiary, Z. et al. Microparticles containing erlotinib-loaded solid lipid nanoparticles for treatment of non-small cell lung cancer. *Drug Dev. Ind. Pharm.* **43** (8), 1244–1253 (2017).
26. Cao, J. et al. Investigation on the interaction behavior between curcumin and PAMAM dendrimer by spectral and docking studies. *Spectrochim. Acta Part A Mol. Biomol. Spectrosc.* **108**, 251–255 (2013).
27. Danaei, M. et al. Impact of particle size and polydispersity index on the clinical applications of lipidic nanocarrier systems. *Pharmaceutics* **10** (2), 57 (2018).
28. Wang, L. et al. Encapsulation of curcumin within poly (amidoamine) dendrimers for delivery to cancer cells. *J. Mater. Science: Mater. Med.* **24** (9), 2137–2144 (2013).
29. Maher, D. M. et al. Curcumin suppresses human papillomavirus oncoproteins, restores p53, rb, and ptpn13 proteins and inhibits benzo [a] pyrene-induced upregulation of HPV E7. *Mol. Carcinog.* **50** (1), 47–57 (2011).
30. Aggarwal, B. B., Kumar, A. & Bharti, A. C. Anticancer potential of curcumin: Preclinical and clinical studies. *Anticancer Res.* **23** (1/A), 363–398 (2003).
31. Anand, P. et al. Bioavailability of curcumin: Problems and promises. *Mol. Pharm.* **4** (6), 807–818 (2007).
32. Curcio, M. et al. Facile synthesis of pH-responsive polymersomes based on lipidized PEG for intracellular co-delivery of curcumin and methotrexate. *Colloids Surf., B.* **167**, 568–576 (2018).
33. Majidzadeh, H. et al. PAMAM dendrimers based co-delivery of methotrexate and berberine for targeting of hela cancer cells. *Toxicol. Rep.* **13**, 101765 (2024).

34. Mujokoro, B. et al. Combination and co-delivery of methotrexate and curcumin: Preparation and in vitro cytotoxic investigation on glioma cells. *J. Pharm. Innov.* **15**, 617–626 (2020).
35. Kheiriabad, S. et al. Applications of advanced nanomaterials in biomedicine, pharmaceuticals, agriculture, and food industry. *BioNanoScience* **14**, 4298–4321 (2024).
36. Vakilinezhad, M. A. et al. Methotrexate and Curcumin co-encapsulated PLGA nanoparticles as a potential breast cancer therapeutic system: in vitro and in vivo evaluation. *Colloids Surf., B.* **184**, 110515 (2019).
37. Syed, A. et al. Multifunctional nanoparticles encapsulating methotrexate and curcumin for holistic management of rheumatoid arthritis: In-vitro and pre-clinical assessment. *Drug Dev. Ind. Pharm.* **49** (8), 536–549 (2023).
38. Danafar, H. et al. Co-delivery of methotrexate and curcumin with mPEG-PCL polymeric nanoparticles and evaluation of toxicity effect on MCF7 breast cancer cell line. *Inorg. Chem. Commun.* **142**, 109715 (2022).
39. Mukherjee, S. P. et al. Mechanistic studies of in vitro cytotoxicity of poly (amidoamine) dendrimers in mammalian cells. *Toxicol. Appl. Pharmcol.* **248** (3), 259–268 (2010).
40. Mousazadeh, N. et al. Anticancer evaluation of methotrexate and curcumin-coencapsulated niosomes against colorectal cancer cell lines. *Nanomedicine* **17** (4), 201–217 (2022).

Acknowledgements

The authors are thankful to Tabriz University of Medical Sciences for supporting this project (grant No: 59561). Also, we want to give a special thanks to Dr. Salar Hemmati due to its help in interpretation of FT-IR results.

Author contributions

S.K. Prepare drug loaded PAMAM, carry out its characterization, perform DAPI staining assay and flow cytometry and writing original draftA.A. conjugate MTX-NHS to PAMAM and perform drug releaseM.G. perform cytotoxicity and DATA analysisS.N.A. Do conceptualizationN.G perform ROS level measurement .J.E.N.D. supervise this study and writing - review & editing of articleH.A. carry out SEM and writing - review & editingM.R.H supervise this study and writing - review & editing of article.

Funding

This research was funded by National Natural Science Foundation of China [No. 82074166, 81473496], Huadong Medicine Joint Funds of the Zhejiang Provincial Natural Science Foundation of China [No. LHDMZ24H050001].

Declarations

Competing interests

The authors declare no competing interests.

Additional information

Correspondence and requests for materials should be addressed to J.E.N.D., H.A. or M.R.H.